Indirect Vector Controlled Induction Motor Drive Better Performance and Analysis with A New Modified MPPT Controller in Interfacing with dSPACE DS 1104

[1]B. Pakkiraiah, Student Member, IEEE [2]G. Durga Sukumar
[1,2]Department of Electrical and Electronics Engineering,
[1,2]Vignan's Foundation for Science Technology and Research University,
[1,2]Guntur, A.P, India-522213.
Email:[1]pakki1988@gmail.com *Email:[2]durgasukumar@gmail.com*

***Abstract*--Due to the increase in power demand the earth natural resources are depleting day by day and renewable energy sources have become an important alternate and solar energy is mainly used. In order to track the radiations from the sun in an efficient manner the maximum power point tracking (MPPT) controller is used. But the existed MPPT controllers were developed based upon the ideal characteristics of constant irradiation and temperature. To overcome the above problem a practical data is considered for designing of MPPT controller which is based upon variable irradiance under variable temperatures. The output obtained from the MPPT is given to the boost converter with an inverter to find the performance of an indirect vector controlled induction motor drive under different operating conditions. For inverter control, a SVM algorithm in which the calculation of switching times is proportional to the instantaneous values of the reference phase voltage. It eliminates the calculation of sector and angle information. The torque ripple and the performance of induction motor drive with ideal and practical data with proposed MPPT are compared under different operating conditions. An experimental validation is carried out with the dSPACE DS 1104 and the comparison is made with the simulation results.**

***Keywords*-- indirect vector controlled, induction motor drive, maximum power point tracking, space vector modulation, torque ripple, total harmonic distortion, variable irradiance and variable temperature.**

1. Introduction

Among the renewable energy sources, the energy through the solar photovoltaic system can be considered the most prerequisite sustainable resource because of ubiquity. However the transfer of energy resulting from photovoltaic conversion remains relatively weak. Therefore the tracking control strategies have to be proposed for the PV system to avoid non linear V-I and V-P characteristics of PV module [1-3]. The loss of energy conversion is not only in the PV system also with the loads connected to the PV systems with. The criterion of reducing such loss mainly depends on DC-DC switched mode converters maintaining isolation to the connected load by providing of maximum operating voltage V_{MPP} with the help of a MPPT controller [4]. An analog circuitry based MPPT controller with the sliding mode controllers introduced to enhance the output and to get better performance under dynamic conditions have been presented [5]. The output voltage is sampled several times for switching frequency to oversample the ratio. Here multiple sampling is used to reduce the phase lag as the last sampling instant and the time of switching can be no longer. In multi sampled case PI controller is used for higher controller bandwidths. These circuits are seems to be more susceptible to limit cycle oscillations [6].

A fast and unconditionally stable maximum power point tracking is introduced to attain the fast dynamics and all range stability by the sliding mode control to acquire high tracking efficiency. The controller can operate as a voltage source or a current source maintaining stability all across the photo voltaic curve which is analyzed by using the stability region method [7-8]. The sliding mode MPPT controller is to study the performance on a synchronous SEPIC converter. And its extension to various classes of dc/dc converters has been studied. The dynamic response of a MPP tracker can be improved by constant frequency PWM controller [9]. Neural network and fuzzy logic based MPPT controller is used to extract maximum available power from PV panel to boost converter to reduce the over shooting, time response and oscillations in increasing the stability and efficiency of the system [10].

A MPPT controller with the inverter is connected to the indirect vector control induction motor drive with space vector modulation technique to get the better performance due to PV system. Various strategies for selecting the order of vectors with zero vectors to reduce the harmonic content and the switching losses [11-12]. The fault tolerant operation of a high power 7-level CHB inverter is implemented based on SVM algorithm. Here the inverter drives medium voltage 2.3 KV/2250 hp induction motor using rotor flux oriented control strategy. The indirect rotor flux oriented control is used for induction motors to achieve good dynamic performance [13]. The space vector modulation diagram of a inverter is composed of number of sub hexagons. The sector identification can be done by determining the triangle which encloses the tip of the reference space vector diagram with forming of six regions [14-15].

To overcome the distortions in the output voltage and currents of multi level inverter (MLI) the single phase SVM based CHBMLI is introduced for PV system to improve the

quality of power even under non ideal conditions [16]. The relationship between SVM and carrier based PWM are observed to achieve SVM's performance with the use of carrier based PWM. Common mode injection technique is used in carrier based PWM to develop SVM. Because SVM technique is the popular one due to its simplicity and better performance at low modulation ratio. Some times SVM technique becomes difficult to achieve when the number of levels increases [17]. Fuzzy logic controller gives the superior dynamic and steady state performance compared to PI controller [18]. A torque ripple and better performance is obtained with the help of genetic algorithm-particle swarm optimization based indirect vector control for optimal torque control of induction motor [19]. A comparison of neuro fuzzy based space vector modulation with neural network and conventional based system has been presented [20]. In this paper, section 2 explains about the mathematical modeling of solar PV array. Section 3 describes the overview of proposed MPPT algorithm. Section 4 discusses the modeling of induction motor and indirect vector control. Section 5 explains about the proposed SVM for two level inverter. Matlab-simulation & experimental results are presented in section 6 and the concluding remarks are stated in section 7.

2. Mathematical modeling of solar PV array

Photovoltaic technology converts solar energy directly into electricity through solar cells. A photovoltaic generator, also known as a photovoltaic array, is the total system consisting of all PV modules connected in series or parallel with each other. A solar cell constitutes the basic unit of a PV generator which in turn, is the main component of a solar generator. For a photo voltaic system power generated is calculated as $P = V. I$

Where P representing power in watts (W), V the voltage in volts (V), and I the current in ampere (A). Fig. 1 shows a model of a solar cell equivalent circuit.

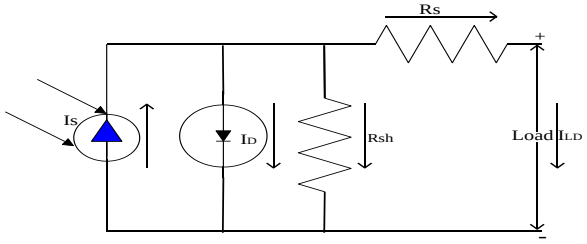

Fig. 1 model of solar cell equivalent circuit.

$$I_{LD} = I_S - I_D - I_{sh} \quad (14)$$

Where I_S refers to the sun light current and I_D is the diode current.

From the Shockley equation, the diode current can be expressed as

$$I_D = I_0[\exp\left(\frac{q(V_{LD}+I_{LD}R_s)}{\gamma K T_s}\right) - 1] \quad (15)$$

Where I_0 refers to actual reverse saturation current, q electron charge, γ, K are the shape factor and Boltzmann Constant

Substituting (15) in (14)

$$I_{LD} = I_S - I_0[\exp\left(\frac{q(V_{LD}+I_{LD}R_s)}{\gamma K T_s}\right) - 1] \quad (16)$$

Where $\gamma = Z. N_A. N_{SC}$

Z is the completion factor, N_A is the number of modules in an array, N_{SC} is the number of series connected cells.

$$I_S = \frac{G}{G_R}\left(I_{SCR} + \mu_{SCR}\ (T_S - T_{SCR})\right) \quad (17)$$

In the equations above, I_{SCR} refers to the sun light current at reference condition; G, G_R the irradiance, actual and at reference condition respectively, μ_{SCR} the manufacturer supplied temperature coefficient of short-circuit current, T_S , T_{SCR} the solar cell temperatures actual and reference condition respectively and

$$I_O = I_{OR}\left(\frac{T_S}{T_{SCR}}\right)^3 \exp\left[\left(\frac{q\varepsilon_G}{k\ Z}\right)\left(\frac{1}{T_{SCR}} - \frac{1}{T_{CS}}\right)\right]$$

I_{OR} refers to reverse saturation current at reference condition

The module photo current I_S of the photovoltaic module depends linearly on the solar irradiation and is also influenced by the temperature according to the equation (17). The value of module short-circuit current I_{SCR} is taken from the data sheet of the reference model.

3. Proposed maximum power point tracking

Maximum power point tracking control technique is used mainly to extract maximum capable power of the PV modules with respective solar irradiance and temperature at particular instant of time by Maximum Power Point Tracking Controller. A number of algorithms are developed to track the maximum power point efficiently. Most of the existing MPPT algorithms suffer from the drawback of being slow tracking. Due to which the utilization efficiency is reduced. There are several types MPPT Control techniques to improve the solar energy efficiency such as Incremental Conductance (INC), Hill Climbing or Perturbation & Observation (P&O) are the most conventionally used methods.

The appearance of multi peak output curves of partial shading in PV arrays is common, where the development of an algorithm for accurately tracking the true MPPs of the complex and non-linear output curves is crucial. A typical solar panel converts only 30-40 percent of the incident solar irradiation into electrical energy. Maximum power point tracking is used to increase the efficiency of the panel. The requirement to get the maximum power is that the source resistance should be equal to that of the load resistance. In the source side, a boost converter is connected to a solar panel in order to enhance the output voltage so that to use for different applications like motor loads by changing the duty cycle of the boost converter

The proposed MPPT algorithm takes the practical obtained values from the PV array i.e V, I_L and calculates the maximum tracked available power P_1. This calculated power P_1 is considered as a initial reference value in the algorithm for this iteration. After a time instant 0.01 seconds it takes another set of values V & I_L and calculates P2. After P1 and

P2 differential power dp = P2-P1 is calculated. This calculated dP is used for the formation of duty cycle D and this can be used for providing of gating pulse for boost converter. For the next iteration P2 is consider initial reference and the process is repeated. The flow chart for the algorithm is given in Fig. 2

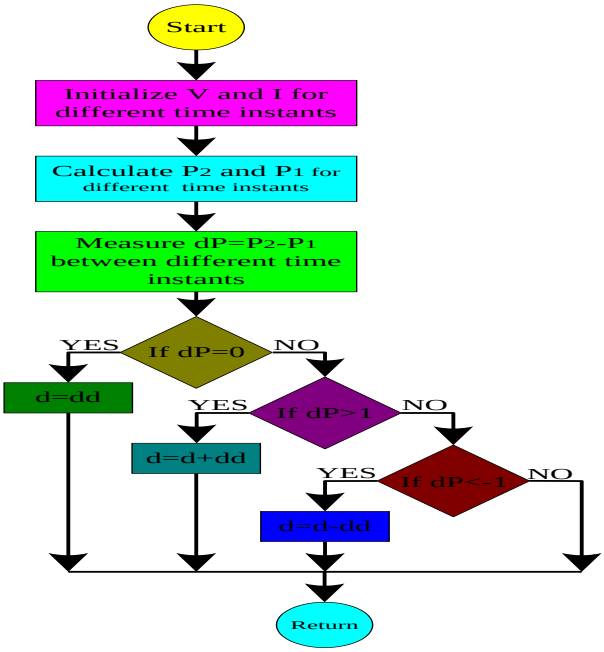

Fig.2 Flow chart of proposed MPPT Controller

Where dd is the differential duty ratio corresponding to the differential power of particular iteration and d is the duty ratio of the prior time instant.

From the proposed MPPT controller it is observed that $I_S >> I_O$ and that the Maximum Power Point current I_{MPP} is also calculated at MPP with thermal voltage is

$$I_{MPP=}I_S - I_O e^{\left(\frac{V_{MPP}}{V_{TH}}\right)} \quad (19)$$

Then I_O becomes as

$$I_O = \frac{I_{SCR}}{e^{\left(\frac{V_{OC}}{V_{TH}}\right)}} \quad (20)$$

With the consideration of V_{OC} and V_{TH} the calculation of I_{MPP} is

$$I_{MPP} = I_{SCR}\left[1 - e^{\left(\frac{V_M - V_{OC}}{V_{TH}}\right)}\right] \quad (21)$$

Then the thermal voltage V_{TH} is calculated as

$$V_{TH} = \frac{V_{MPP} - V_{OC}}{ln\left(\frac{I_{SCR} - I_{MPP}}{I_{SCR}}\right)} \quad (22)$$

So Array power can be calculated as

$$P_{ARRAY} = V_{MPP} \times I_{MPP} = I_S \times V - I_O[e^{\left(\frac{V}{V_{TH}}\right)} - 1] \times V \quad (23)$$

From this by deriving the above equation w.r.t. the voltage we get the maximum array power as

$$P_{ARRAY\ MAX} = \frac{\partial P_{ARRAY}}{\partial V} = I_O\left[e^{\left(\frac{V}{V_{TH}}\right)} - 1\right] + I_O \times \frac{V}{V_{TH}}\left[e^{\left(\frac{V}{V_{TH}}\right)} - 1\right] \quad (24)$$

From above equation we are observing for the maximum voltage that gives the maximum array power is $V=V_{MPP}$. So that

$$\frac{\partial P_{ARRAY}}{\partial V}\ at\ V = V_{MPP} = 0 \quad (25)$$

Then it gives the

$$I_{MPP} - \frac{V_{MPP}}{V_{TH}} \times I_D = 0 \quad (26)$$

a. Practical Outputs of PV Module with Conventional and Proposed MPPT at Standard Test Conditions (STC)

Under Standard Test Conditions, the irradiance provided is 1000 W/m^2 and temperature is about 25^{o}C. During this the results obtained with conventional and proposed MPPT are shown in Fig. 3. Here the maximum power point voltage V_{MPP} and current I_{MPP} with the proposed MPPT are obtained as 30.7 Volts and 8.13 Amps respectively.

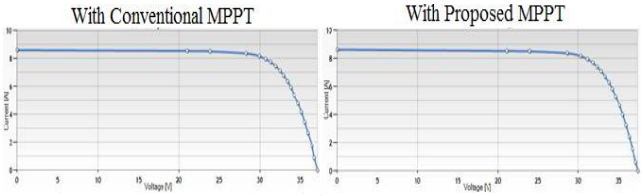

Fig. 3 Practical I-V characteristics of PV module with conventional and proposed MPPT controller at Standard Test Conditions (STC)

b. Practical outputs of PV Module with the Proposed MPPT at Variable Irradiance and Constant Temperature

When both the temperature and irradiance are variable then it increases the array current and slightly increases the voltage till the irradiance rise and vice-versa. These results are available in Fig. 4

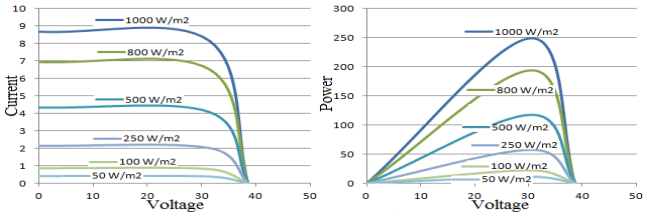

Fig. 4 Practical I-V & P-V characteristics of PV module with variable irradiance and constant temperature

c. Practical outputs of PV Module with the Proposed MPPT at Variable Irradiance and Variable Temperature

When both the temperature and irradiance are variable then it increases the array current and slightly increases the voltage till the irradiance rise and vice-versa. Also it increases the PV module current and decreases the voltage till the temperature rise and vice-versa. These results are presented in Fig. 5

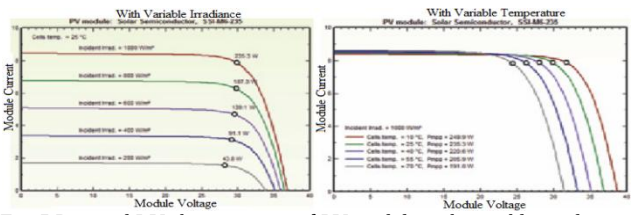

Fig. 5 Practical I-V characteristics of PV module with variable irradiance and variable temperature

4. Modeling of induction motor and indirect vector control

The mathematical model of a three-phase, squirrel-cage induction motor can be described in stationary reference frame as

$$V_{qs} = (R_S + pL_{ss})i_{qS} + pL_m i_{qR} \quad (1)$$

$$V_{ds} = (R_S + pL_S)i_{dS} + pL_m i_{dR} \quad (2)$$

$$0 = pL_m i_{qS} - \omega_R L_m i_{dS} + (R_R + pL_R)i_{qR} - \omega_R L_R i_{dR} \quad (3)$$

$$0 = \omega_E L_m i_{qS} + pL_m i_{dS} + \omega_R L_R i_{qR} + (R_R + pL_R)i_{dR} \quad (4)$$

Where $\omega_R = \frac{d\theta}{dt}$, $p = \frac{d}{dt}$

Suffixes s and r represents stator and rotor respectively

V_{dS} and V_{qS} are d-q axis stator voltages respectively,

i_{dS}, i_{qS} and i_{dR}, i_{qR} are d-q axis stator currents and rotor currents respectively,

R_S and R_R are stator and rotor resistances per phase respectively,

L_S, L_R are self inductances of stator and rotor and L_m is mutual inductance

Stator and rotor flux linkages can be expressed as in-terms of inductances as

$$\lambda_{qS} = L_S i_{qS} + L_m i_{qR} \quad (5)$$

$$\lambda_{dS} = L_S i_{dS} + L_m i_{dR} \quad (6)$$

$$\lambda_{qR} = L_R i_{qR} + L_m i_{qS} \quad (7)$$

$$\lambda_{dr} = L_R i_{dR} + L_m i_{dS} \quad (8)$$

From the above equations (1)-(4), Squirrel-cage induction motor can described by following equations in stator reference frame as

$$\begin{bmatrix} V_{qS} \\ V_{dS} \\ 0 \\ 0 \end{bmatrix} = \begin{bmatrix} R_S + pL_S & 0 & pL_m & 0 \\ 0 & R_S + pL_S & 0 & pL_m \\ pL_m & -\omega_R L_m & R_R + pL_R & -\omega_R L_R \\ \omega_R L_m & pL_m & \omega_R L_R & R_R + pL_R \end{bmatrix} \begin{bmatrix} i_{qS} \\ i_{dS} \\ i_{qR} \\ i_{dR} \end{bmatrix} \quad (9)$$

The electromagnetic torque Te of the induction motor is given by

$$T_e = \frac{3}{2}\left(\frac{p}{2}\right)\left(\lambda_{qR} i_{dR} - \lambda_{dR} i_{qR}\right) \quad (10)$$

From the dynamic model of induction machine, the rotor flux is aligned along the d-axis then the q-axis rotor flux λ_{qR}=0. So from the equations (7) and (10) described in the previous section and putting λ_{qR}=0, the electromagnetic torque of the motor in the indirect vector control can be expressed in indirect vector control as

$$T_e = \frac{3}{2}\left(\frac{p}{2}\right)\frac{L_m}{L_R}\left(\lambda_{dR} i_{qS}\right) \quad (11)$$

If the rotor flux linkage λ_{dR} is not disturbed, the torque can be independently controlled by adjusting the stator q component current i_{qS}.

As the rotor flux aligned on d-axis, this leads to λ_{qR}=0 and λ_{dR}=λ_R, then

$$\omega_{Sl} = \frac{L_m R_R}{\lambda_R L_R} i_{qS} \quad (12)$$

The rotor angle θ_e is estimated using the measured rotor speed ω_r and slip speed ω_{Sl}

$$\theta_e = \int \omega_e dt = \int (\omega_R + \omega_{Sl}) dt = \theta_R + \theta_{Sl} \quad (13)$$

5. Proposed SVM for two level inverter

SVM is applied to minimize the overall switching changes when the nearest three space vectors are used. The identical properties of switching states and their redundancies enable the improvement of the SVM technique in order to reduce the switching loss and operating under fault conditions. In PWM technique each phase voltage is produced separately according to its reference, while SVM technique transforms three phase reference voltage into a rotational vector in space vector domain and synthesizes it through the appropriate switching sates of the inverter. Through this strategy it is possible to use the redundancy in switching states to minimize the converter loss and to operate under fault conditions.

In this the space vector modulation algorithm for two level inverter is introduced for which the solar panels are connected to provide the dc supply. SVM basic principle and switching sequence is given in order to get symmetrical algorithm pulses and voltage balancing. This scheme is used to control the output voltage of the two level inverter with the MPPT controller. In the SVM algorithm, the d-axis and q-axis voltages are converted into three-phase instantaneous reference voltages. Then the imaginary switching time periods proportional to the instantaneous values of the reference phase voltages which are defined as

$$T_{uS} = \left(\frac{T_S}{V_{DC}}\right)V_{uS}^* , T_{vS} = \left(\frac{T_S}{V_{DC}}\right)V_{vS}^* , T_{wS} = \left(\frac{T_S}{V_{DC}}\right)V_{wS}^* \quad (27)$$

Where T_S and V_{DC} are the sampling interval time and dc link voltage respectively. Here, sampling frequency is the twice the carrier frequency. The maximum (*Max*), middle (*Mid*) and minimum (*Min*) imaginary switching times can be found in each sampling interval by using (28) - (30).

$$T_{Max} = Max(T_{u1}, T_{v1}, T_{w1}) \quad (28)$$

$$T_{Min} = Min(T_{u1}, T_{v1}, T_{w1}) \quad (29)$$

$$T_{Mid} = Mid(T_{u1}, T_{v1}, T_{w1}) \quad (30)$$

The active voltage vector switching times T_1 and T_2 are calculated as

$$T_1 = T_{Max} - T_{Mid} \text{ and } T_2 = T_{Mid} - T_{Min} \quad (31)$$

The zero voltage vectors switching time is calculated as

$$T_z = T_S - T_1 - T_2 \quad (32)$$

The zero state time will be shared between two zero states as T_0 for V_0 and T_7 for V_7 respectively, and can be expressed as [31].

$$T_0 = K_0 T_Z \quad (33)$$

$$T_7 = (1 - K_0)T_Z \quad (34)$$

The various SVM algorithms can be generated by changing k_o between zero and one. However, in this SVM algorithm, the zero voltage vector time distributed equally among V_0 and V_7. Hence, here k_0 is taken as 0.5 to obtain the SVM algorithm.

5.1 Block diagram of vector control induction motor

The block diagram of the proposed indirect vector controlled induction motor drive with two-level inverters is as illustrated in Fig. 6. From the field control and speed control the reference values of currents i_{d1}^* and i_{q1}^* are obtained and these values are compared with the respective i_{d1} and i_{q1} currents generated by the transformation of phase currents with the unit vector. From the respective errors, d-axis voltage V_d and q-axis voltage V_q are generated through PI controllers. These voltages are then converted into stationary frame and then given to SVM block.

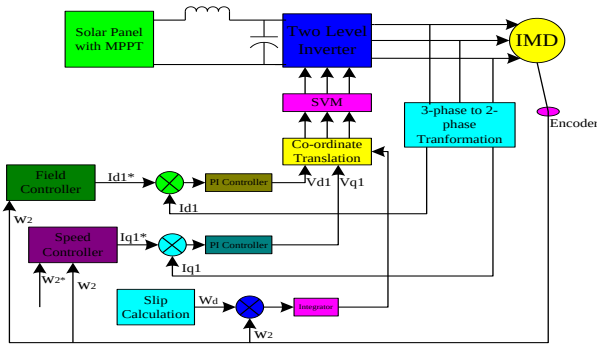

Fig. 6 Vector control of motor with proposed MPPT technique

6. Results and discussion

a) Theoretical and Practical characteristics of PV array with variable irradiance and constant temperature

When irradiance is considered, PV current and voltage increases with respect to the irradiance rise. Comparing to theoretical values practical output values have drooping nature due to variable irradiance for instant to instant. The observations voltage, current and power are available in Fig. 7 (a&b).

b) Theoretical and Practical calculated readings of PV array with variable temperature and constant irradiance

Considering variable temperature and constant irradiance, the PV array current increases with increase in temperature and vice-versa. And voltages decreases drastically decreases with increase in temperature and vice-versa. The calculated values with the experimental validation from 8 A.M to 5.30 P.M are illustrated in Fig. 8 (a&b).

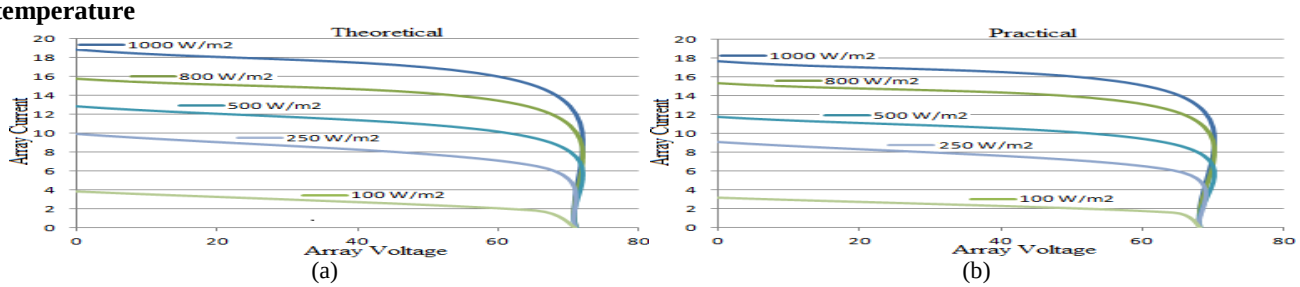

(a) (b)

Fig. 7 V-I characteristics of an array at different instants a) Theoretical b) Practical

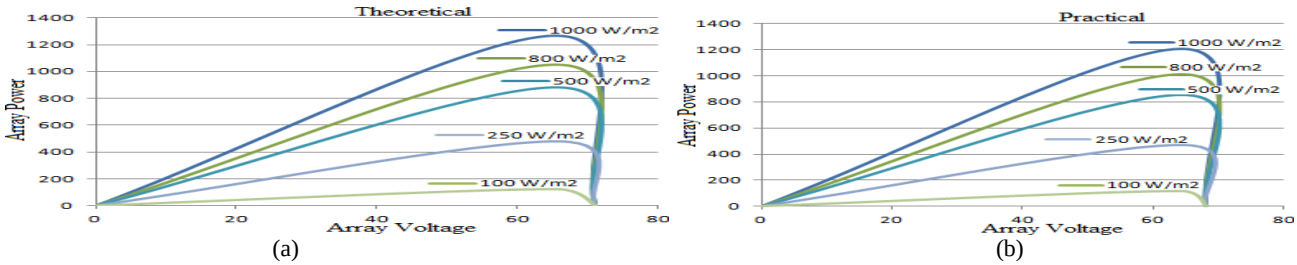

(a) (b)

Fig. 8 P-V characteristics of an array at different instants a) Theoretical b) Practical

c) Theoretical and Practical readings of PV array with variable irradiance and variable temperature

In practical working conditions maintaining of constant temperature and irradiance is not possible these are going to vary from instant to instant. Considering variable irradiance and temperature the following values are calculated with the experimental validation from 8 A.M to 5.30 P.M shown in Fig. 9-10

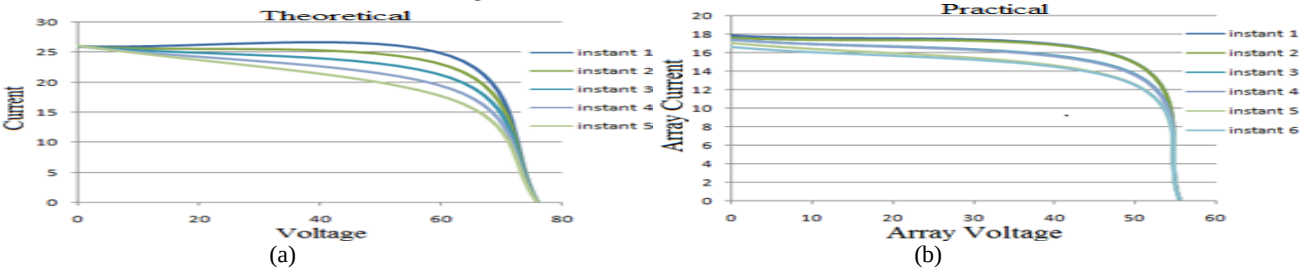

(a) (b)

Fig. 9 I-V characteristics of an array at variable irradiance and variable temperature a) Theoretical b) Practical

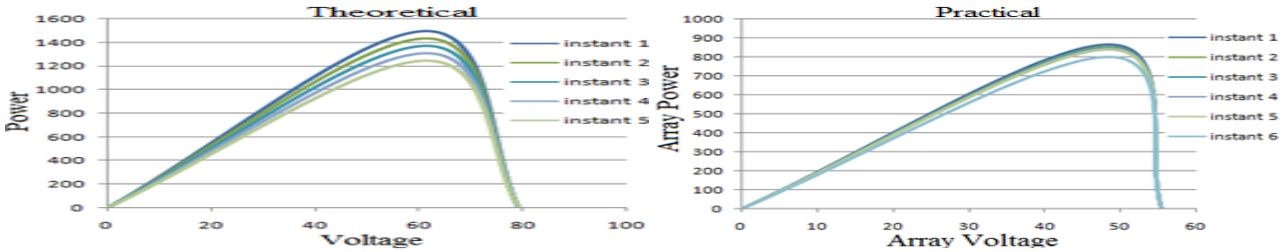

(a) (b)

Fig. 10 P-V characteristics of an array at variable irradiance and variable temperature a) Theoretical b) Practical

TABLE.1
THEORETICAL AND PRACTICAL VALUES OF IRRADIANCE, VOLTAGE, CURRENT AND POWER FOR VARIABLE TEMPERATURE AND IRRADIANCE

Time in (am/pm)	Temperature in (^{0}C)	Irradiance in (W/m^2)	Voltage in (Volts)		Current in (Amps)		Power in (Watts)	
			Theoretical	Practical	Theoretical	Practical	Theoretical	Practical
08.00	30.75	143.55	66.48	60.90	3.9010	3.81	259.33	232.02
08.30	32.55	285.64	68.42	61.60	7.4060	7.72	478.94	475.55
09.06	33.35	408.50	69.43	62.30	10.6036	10.93	695.68	680.93
09.30	35.25	475.73	69.86	63.80	12.3547	12.41	815.96	791.75
10.00	38.25	494.11	69.95	64.20	12.8358	12.83	848.49	823.68
10.30	39.35	513.48	70.05	64.70	13.3409	13.22	883.33	855.33
11.00	39.55	552.65	70.27	65.20	14.3609	14.12	954.96	920.62
11.30	40.02	605.10	70.53	65.80	15.7270	15.33	1048.07	1008.71
12.00	40.50	631.65	70.65	66.10	16.4187	15.91	1096.48	1051.65
12.10	40.68	666.39	70.81	66.40	17.3233	16.71	1159.15	1109.54
12.30	41.10	695.60	70.93	67.30	18.0843	17.22	1212.19	1158.90
13.00	41.35	724.29	71.05	68.10	18.8315	17.73	1264.69	1207.41
13.30	40.45	666.39	70.81	66.80	17.3230	16.62	1159.15	1110.21
14.00	40.08	608.13	70.54	65.70	15.8057	15.43	1053.86	1013.75
14.30	39.00	552.75	70.27	64.30	14.3630	14.31	953.56	920.13
15.00	38.42	479.56	69.86	63.80	12.4570	12.51	822.25	798.13
15.30	37.95	384.05	69.22	63.20	9.9703	10.12	652.05	639.58
16.00	37.32	308.32	68.59	61.70	7.9986	8.32	518.54	513.34
16.30	37.06	147.91	66.46	59.70	3.8229	3.98	240.73	237.60
17.08	33.25	74.63	64.55	58.40	1.9149	2.06	122.74	120.30
17.30	32.85	28.84	61.79	57.90	0.7235	0.79	46.35	45.74

d) PV array characteristics with conventional and proposed MPPT Techniques

From the observation of conventional and proposed MPPT technique I-V and P-V characteristics it is observed that the conventional MPPT current obtained is 17.70 Amps where as the proposed MPPT current is about is 18.83 Amps. Similarly the conventional MPPT voltage and the power are found as 68.10 Volts and 1205.37 Watts with that of the proposed MPPT voltage and the power are about 72.74 Volts and 1366.76 Watts. These results are presented in Fig. 11-13.

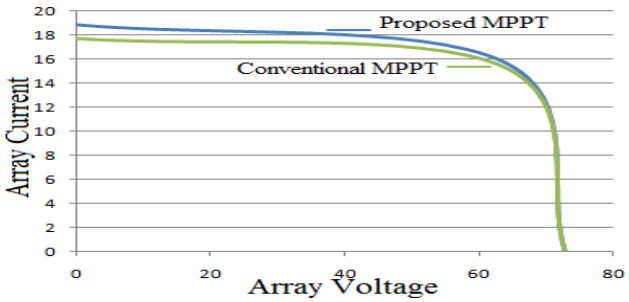

Fig. 11 Conventional and Proposed I-V characteristics of PV array

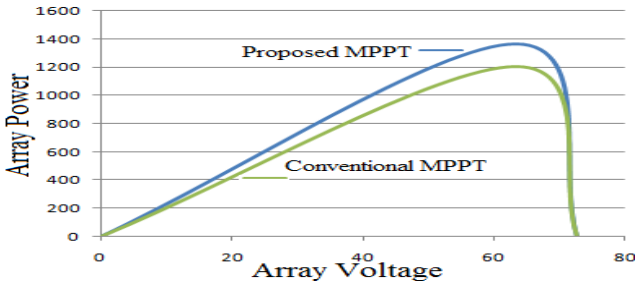

Fig. 12 Conventional and Proposed P-V characteristics of PV array

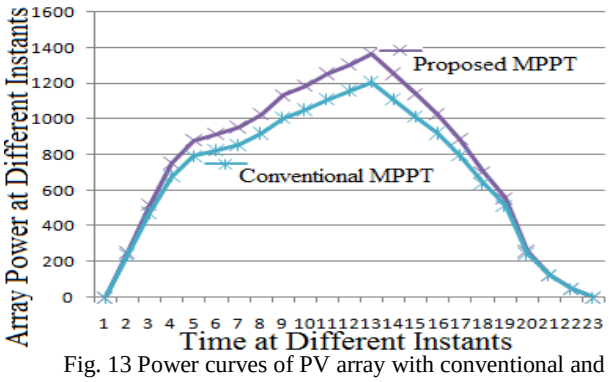

Fig. 13 Power curves of PV array with conventional and proposed MPPT techniques

e) Simulation results of induction motor drive

Simulation results are obtained under different conditions considering the reference value of speed as 1300 rpm and using the switching frequency 5 KHz. The performance of induction motor parameters such as stator phase currents, torque and speed are obtained with the two-level inverter controlled drive are observed in Fig. 14-18.

i) Performance during starting

The performance of the indirect vector controlled induction motor drive during the starting with two-level inverter is shown Fig. 14(a), 14(b) and 14(c). As shown in the figures maximum current during the starting is reduced, the ripple contentment in the torque is reduced, drive reaches steady state earlier in case of proposed MPPT controller. The maximum torque obtained with the conventional MPPT is 13 N-m where as proposed method it is 13.75 N-m. Torque is increased with the proposed MPPT controller. The speed response also reaches steady state earlier with the proposed MPPT than that of conventiosnal method.

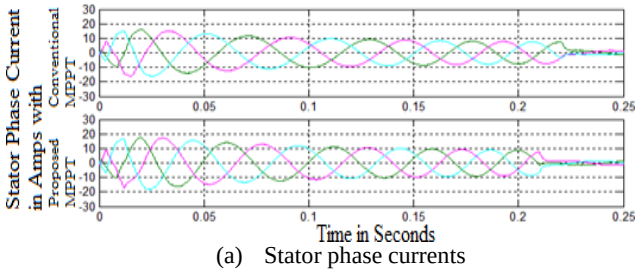

(a) Stator phase currents

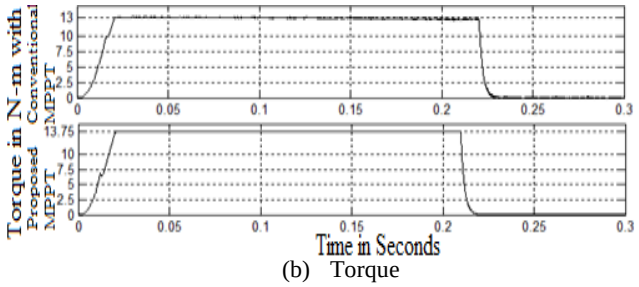

(b) Torque

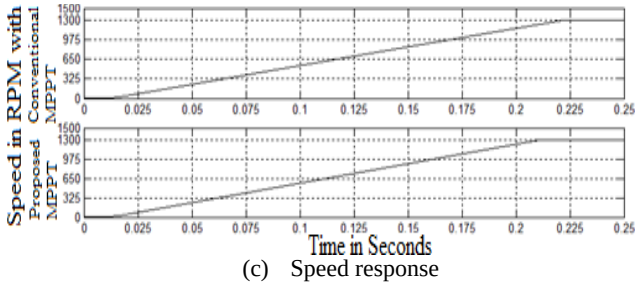

(c) Speed response

Fig. 14 Performance of indirect vector controlled induction motor during starting

ii) Performance during steady state

The steady state phase currents, torque and speed responses of indirect vector controlled drive with two-level inverter are illustrated in Fig. 15(a), 15(b) and 15(c). It is observed that the torque ripple of the two level inverter with the conventional MPPT method is 0.15 where as with the proposed MPPT is 0.03. Lot of ripple improvement is found with the proposed MPPT method. Also the better speed response is obtained with the proposed MPPT compared to conventional method of the indirect vector controlled induction motor drive.

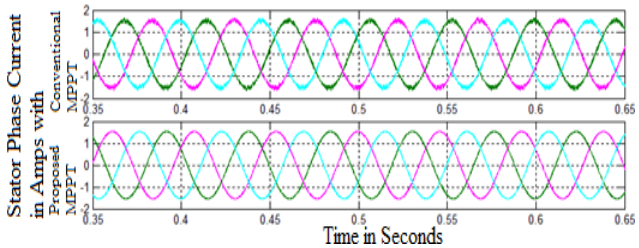

(a) Stator phase currents

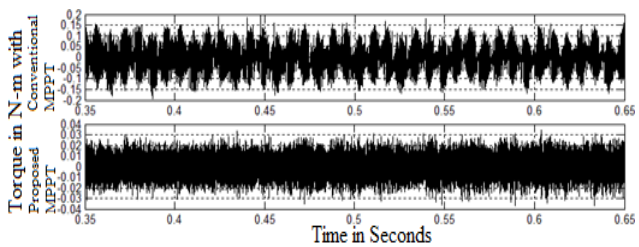

(b) Torque

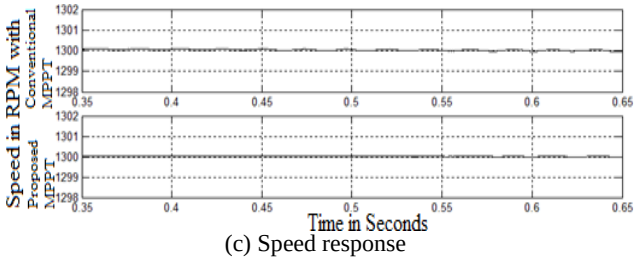

(c) Speed response

Fig.15 Steady state Performance of indirect vector controlled induction motor

iii) Performance during transient step change

The response during the step change in load torque command (the load torque of 8 N-m is applied at 0.7 sec and removed at 0.9 sec) is presented in Fig. 16(a), 16(b) and 16(c). The ripple content in current waveforms and torque is less with the proposed MPPT method of indirect vector controlled induction motor drive. Also the speed decrement is little less with the proposed MPPT during the load change.

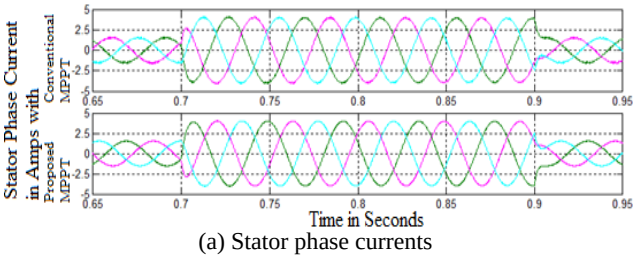

(a) Stator phase currents

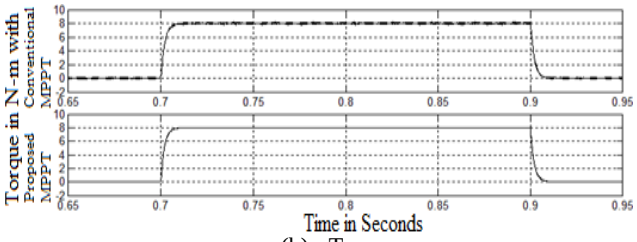

(b) Torque

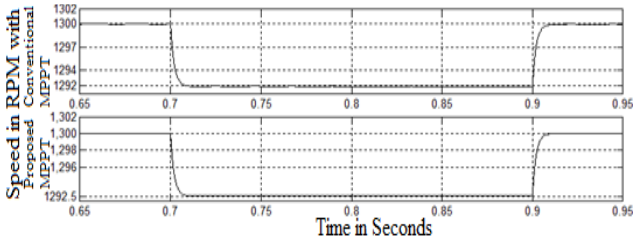

(c) Speed response

Fig.16 Transients during step change in load torque

iv) Performance during transient speed reversal

The results of the drive during speed reversals (From +1300 to -1300 RPM) are available in Fig. 17(a), 17(b) and 17(c). The drive gives less ripple content in the phase currents, torque of an induction motor and speed response reaches the reference value little earlier with the proposed MPPT and experimental validation during the speed reversal.

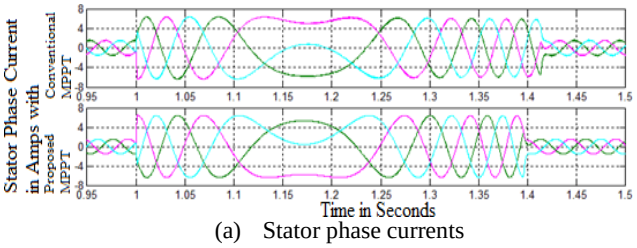

(a) Stator phase currents

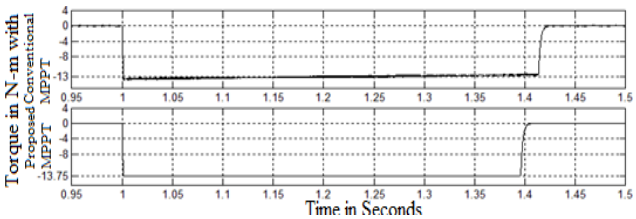

(b) Torque

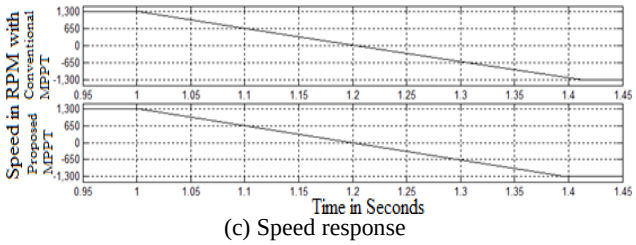

(c) Speed response

Fig. 17 Transients during speed reversal operation (Speed is changed from +1300 rpm to -1300 rpm)

v) Performance during transient speed reversal

The performance of the drive during speed reversals (from -1300 to +1300 RPM) is shown in Fig. 18(a), 18(b) and 18(c). The overall performance of drive is improved with the proposed MPPT and speed response reaches the reference value earlier compared to the conventional MPPT.

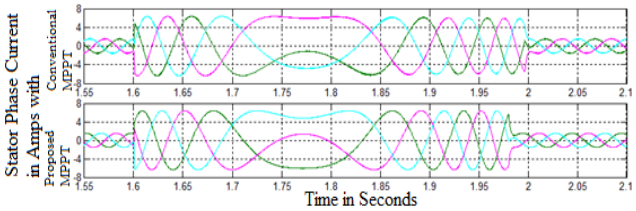

(a) Stator phase currents

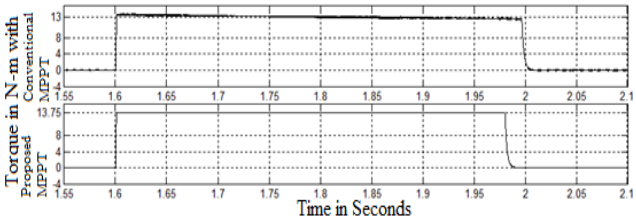

(b) Torque

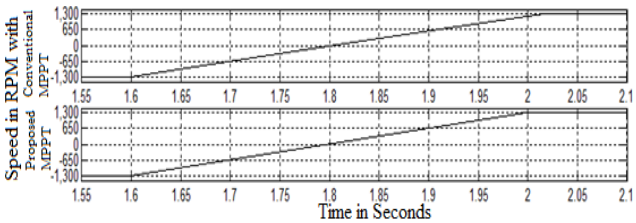

(c) Speed response

Fig. 18 Transients during speed reversal operation (Speed is changed from -1300 rpm to +1300 rpm)

f) Experimental validation results with dSPACE 1104

A dSPACE (DS1104) is used for the real time implementation of vector controlled induction motor drive using the proposed and conventional MPPT Controller. The control algorithm is first developed in Matlab/Simulink. The real time workshop of Matlab generates the C code for the real time implementation. The interface between Matlab and DS1104 allows the controller to be run on the hardware which is an MPC-8240 processor.

In the present case, the optimized C code of the simulink model of the control algorithm is automatically generated by the real time workshop of Matlab in conjunction with the dSPACE hardware, where it is implemented in the real time and the gating pulses are generated. The gating signals for the power switches of the inverter are outputted via the master bit I/Os are available on the dSPACE board. The CLP1104 Connector/Led Combination panel provides easy to use the connections between DS1104 board and the devices is to be connected to it.

The panel also provides an array of LEDs indicating the states of digital signals (gating pulses). The gating pulses are fed to various IGBT driver circuits via the Opto-isolation circuit boards. Sensed signals fed to the ADCs and the generated gating pulses are outputted at master bit I/Os. The block diagram of dSPACE controlled inverter is observed in Fig. 19

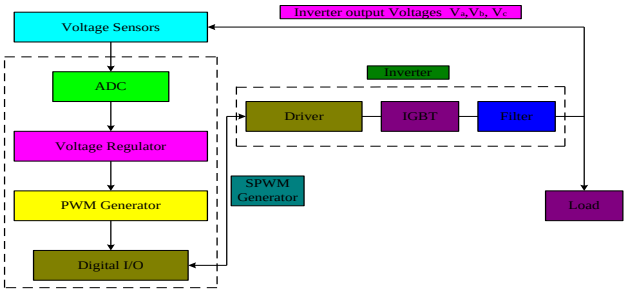

Fig. 19 Block diagram of dSPACE controlled inverter

The schematic diagram gives the clear information of the experimental setup in detail. Here, the speed of the IM is sensed using DC-Vector control. In addition, currents, and the speed of IM are taken into the feedback using sensors via ADC and Mux ADC channels of the DSPACE DS-1104 connector panel. Thereafter, the speed and currents of the IM are estimated and given to the respective controllers. Moreover, the speed and current PI-controllers generate the current and slip speed, respectively as presented in Fig. 20.

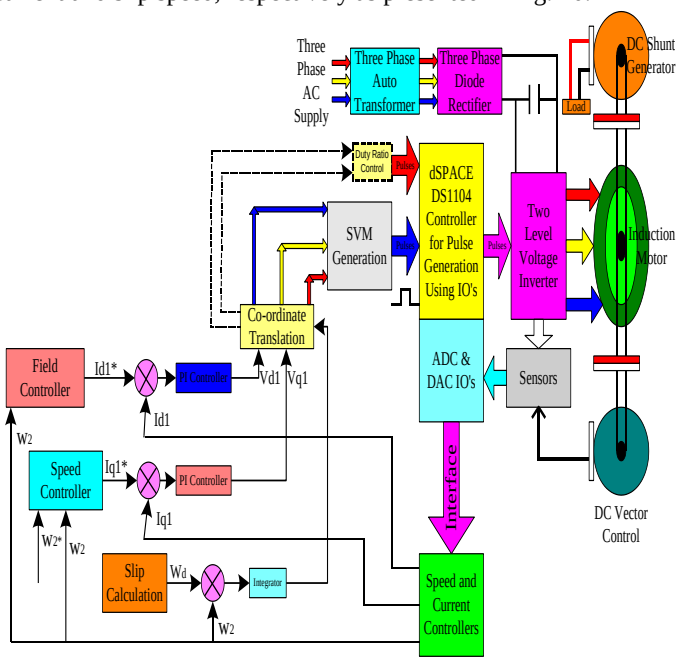

Fig. 20 Vector control of Induction motor with dSPACE DS-1104

Initially, the reference speed set to 1300rpm in both conventional and proposed MPPT of the IM drive at no-load. The PWM pulses are provided to the inverter by a click on the incremental build. The DC-link voltage 500V is applied to the inverter by adjusting three-phase auto-transformer using uncontrolled rectifier. Hence, the IMD picks up its speed up to required value, i.e., 1300rpm and reach to steady state under no-load condition. The corresponding waveforms (torque (T_e), speed (N_r), flux (ψ_e), and current (i_a)) during starting for conventional are taken from the digital storage oscilloscope (DSO) as shown in Fig. 21 (a&b).

Compared to conventional MPPT that thse proposed MPPT has the better percentile ripple improvement in the induction motor parameters during its starting. Such as in torque it is 25%, in flux it is 25%, in current it is 18% and in speed it is about 8% ripple improvement.

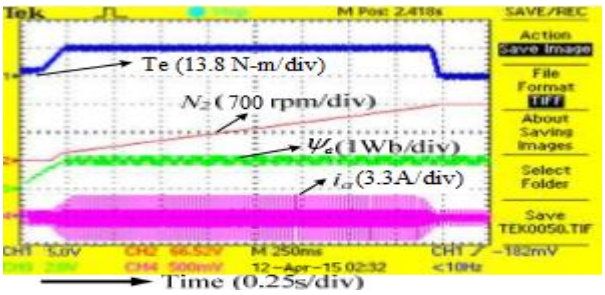

(a)

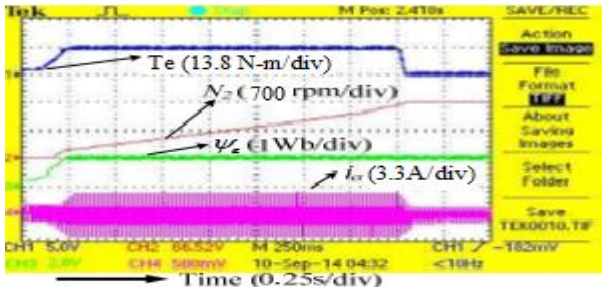

(b)

Fig. 21 starting performance of induction motor a) conventional b) proposed

A sudden load of 8N-m is applied and removed at 0.2s and 0.7s respectively then the corresponding changes in IMD waveforms are shown in Fig. 22 (a&b). The torque and currents suddenly rise/fall due to load perturbation. Proposed MPPT has good ripple improvement from induction motor parameters during load change when compared to the conventional MPPT. Such that it improved in torque about 25%, in flux it is 25%, in current it is 19.33% and in speed it is found to be 8.16%.

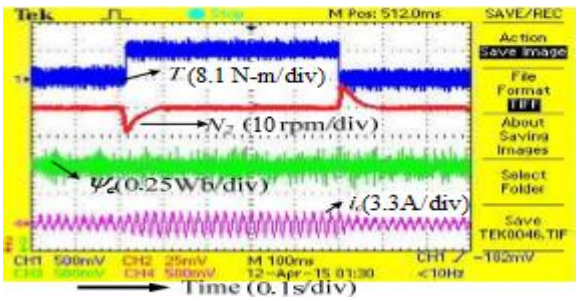

(a)

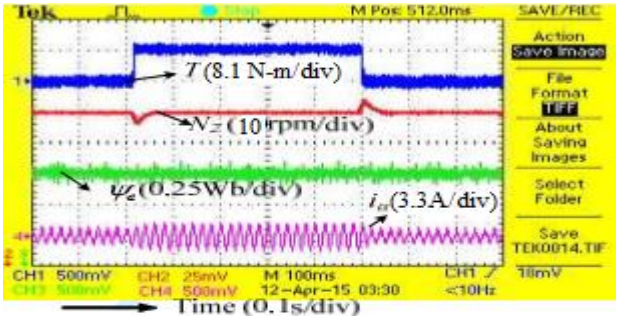

(b)

Fig. 22 performance of induction motor during sudden change in load a) conventional b) proposed

7. Conclusionss

In this MPPT controller for PV system under variable irradiance and variable temperature is presented. The performance of MPPT controller is compared with conventional MPPT controller using indirect vector controlled induction motor drive. The practical characteristic V-I and P-V under variable irradiance and variable temperature and constant temperature with variable irradiance and vice versa are compared with theoretical and practical values. It is observed 20% variation compared to already existed method. From this, the obtained practical values of MPPT controller is developed to obtain better performance when compared to the conventional methods.

The proposed MPPT controller calculates the power of a PV system for every 0.01 seconds and gives the more output. It is observed that it gives 25% more output with the proposed MPPT under variable irradiance and variable temperature. The better dynamic performance of two-level inverter fed induction motor drive is observed under various conditions with the proposed MPPT. For inverter control, SVM algorithm calculates switching times proportional to the instantaneous values of the reference phase voltage, to eliminate the calculation of sector and angle information. The %THD is 25% less compared to with proposed MPPT with SVM algorithm compared to conventional based systems.

Acknowledgement

The funding support given by SERB, Department of Science and Technology (DST), Government of India with vides SERB order No: SERB/ET-069/2013 for the solar based project is acknowledged.

References

[1] T. P. Sahu and T. V. Dixit, "Modeling and analysis of perturb & observe and incremental conductance MPPT algorithm for PV array using cuk converter", *IEEE Students' Conference on Electrical, Electronics and Computer Science (SCEECS)*, pp.1-6, 2014.

[2] M. A. A. Mohd Zainuri, M. A. Mohd Radzi, Azura Che Soh and N. Abdul Rahim, "Comparative Analysis of the perturb-and-observe and incremental conductance MPPT methods", *IEEE 8th International Symposium on Advanced Topics in Electrical Engineering*, pp.1-1, 2013.

[3] B. Pakkiraiah and G. Durga Sukumar, "A New Modified MPPT Controller for Solar Photovoltaic System," *2015 IEEE International Conference on Research in*

Computational Intelligence and Communication Networks (ICRCICN), Kolkata, pp. 294-299, 2015.

[4] M. Adly, M. Ibrahim and H. EI Sherif, "Comparative study of improved energy generation maximization techniques for photovoltaic systems", *IEEE Power and Energy Engineering Conference (APPEEC)*, pp.1-5, 2012.

[5] S. Maity and P. Sahu, "Modeling and analysis of a fast and robust module-integrated analog photovoltaic MPP tracker", *IEEE Transactions on Power Electronics*, vol. no.99, pp.1-1, 2015.

[6] M. Bradley, E. Alarcon and O. Feely, "Design-oriented analysis of quantization-induced limit cycles in a multiple-sampled digitally controlled buck converter", *IEEE Transactions on Circuits and Systems I*, vol.61, no.4, pp.1192-1205, 2014.

[7] Y. Levron and D. Shmilovitz, "Maximum power point tracking employing sliding mode control", *IEEE Transactions on Circuits and Systems I*, vol.60, no.3, pp.724-732, 2013.

[8] E. Bianconi, J. Calvente, R. Giral, E. Mamarelis, G. Petrone, C. A. Ramos-Paja, G. Spagnuolo and M. Vitelli, "A fast current based MPPT technique employing sliding mode control", *IEEE Transactions on Industrial Electronics*, vol.60, no.3, pp.1168-1178, 2013.

[9] E. Mamarelis, G. Petrone and G. Spagnuolo, "Design of a sliding mode controlled SEPIC for PV MPPT applications", *IEEE Transactions on Industrial Electronics*, vol.61, no.7, pp.3387-3398, 2014.

[10] N. Khaldi, H. Mahmoudi, M. Zazi and Y. Barradi, "The MPPT control of PV system by using neural networks based on Newton Raphson method", *IEEE International Renewable and Sustainable Energy Conference (IRSEC)*, pp.19-24, 2014.

[11] J. J. Joshi, P. Karthick and R. S. Kumar, "A solar panel connected multilevel inverter with SVM using fuzzy logic controller", *IEEE International Conference on Energy Efficient Technologies for Sustainability (ICEETS)*, pp.1201-1206, 2013.

[12] M. Aleenejad, H. Iman-Eini and S. Farhangi, "A minimum loss switching method using space vector modulation for cascaded H-bridge multilevel inverter", IEEE *20th International Conference on Electrical Engineering (ICEE)*, pp.546-551, 2012.

[13] M. A. Paymani, M. S. Marhaba and H. Iman-Eini, "Fault-tolerant operation of a medium voltage drive based on cascaded H- bridge inverter", *IEEE Power Electronics Drive Systems and Technologies Conference (PEDSTC)*, pp.551-556, 2011.

[14] C. Sreeja and S. Arun, "A novel control algorithm for three phase multilevel inverter using SVM", *IEEE PES Innovative Smart Grid Technologies-India (ISGT India)*, pp.262-267, 2011.

[15] A. Mbarushimana and Xin Ai, "Real time digital simulation of PWM converter control for grid integration of renewable energy with enhanced power quality", *IEEE Electric Utility Dereglation and Restructing and Power Technologies (DRPT)*, pp.712-718, 2011.

[16] A. Panda, M. K. Pathak and S. P. Srivastava, "An improved power converter for standalone Photovoltaic system", *IEEE Indian Conferene (INDICON)*, pp.1-6, 2013.

[17] Wenxi Yao, Haibing Hu and Zhengyu Lu, "Comparisons of space-vector modulation and carrier-based modulation of multilevel inverter", *IEEE Transactions on Power Electronics*, vol.23, no.1, pp.45-51, 2008.

[18] Minglei Zhou, Kekang Wei, Chenchen Wang, Xiaojie You, Jian Wang and Liwei Zhang, "A rotor flux oriented scheme of induction machine based on voltage controller", *IEEE Industrial Electronics and Applications*, pp.744-748, 2010.

[19] Dong Hwa Kim, "GA-PSO based vector control of indirect three phase induction motor", *Elsevier Science Direct Applied Soft Computing*, vol.7, no.2, pp.601-611, 2007.

[20] Durga Sukumar, Jayachandranath Jitendranath, Suman Saranu, "Three-level Inverter-fed Induction Motor Drive Performance Improvement with Neuro-fuzzy Space Vector Modulation", *Electrical Power Components and Systems*, vol.42, no.15, pp.1633-1646, 2014.